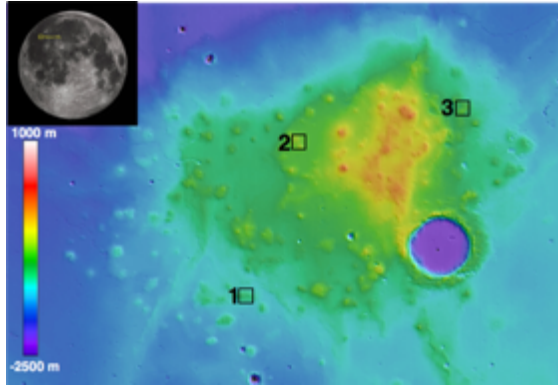


**MAPPING GLASS IN THE MARIUS HILLS VOLCANIC COMPLEX WITH MOON MINERALOGY MAPPER.** M. J. McBride<sup>1</sup>, B. Horgan<sup>1</sup>, and L. R. Gaddis<sup>2</sup>. <sup>1</sup>Purdue University, 610 Purdue Mall, West Lafayette, IN 47907 (mjmcbride@purdue.edu). <sup>2</sup>Astrogeology Science Center, U.S. Geological Survey, Flagstaff, AZ 86001.

**Introduction:** The Marius Hills Volcanic Complex (MHVC) is located on the Moon's near side within Oceanus Procellarum (13.3°N, 47.5°W, Figure 1).



**Figure 1:** A) Location of MHVC on the near side of the Moon. B) Topography of MHVC from LOLA data. Boxes indicate locations of spectra in Figure 3.

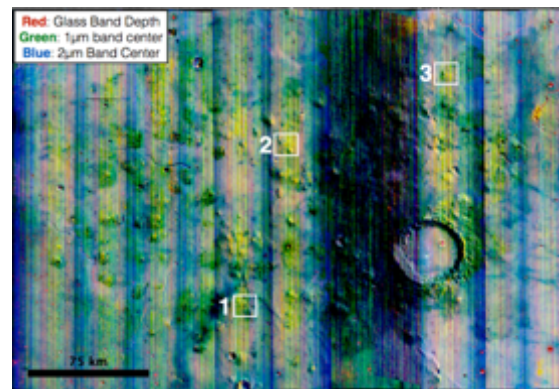
MHVC has a major concentration of volcanic features, including domes, cones, rilles, and lava flows on a plateau 35,000 km<sup>2</sup> in area raised about 100-200 m from the surrounding plains [1, 2]. Gustafson et al. [3] used Clementine color and Lunar Reconnaissance Orbiter (LRO) Narrow Angle Camera (NAC) data for Marius Hills to search for potential lunar pyroclastic deposits but the result was inconclusive. The presence of lunar pyroclastic deposits (LPDs) at MHVC would suggest that explosive volcanic eruptions driven by volatiles were involved in the emplacement of the cones and domes and indicates that lunar eruption styles were more complex than previously thought [e.g., 4]. Iron bearing glass is formed by rapid quenching of magma in explosive eruptions and is a mineralogical indicator of LPDs [5]. Using a new method to map glass and other ferrous minerals [6], we are revisiting the MHVC to search for the presence of glass, to assess the compositional diversity of possible LPDs, and to determine whether explosive volcanism was involved in the emplacement of the observed volcanic features. LPDs were previously thought to be highly homogeneous in composition, but our recent work [7] has shown clear compositional heterogeneity that suggests that eruption styles of these deposits were complex and diverse.

**Background:** Geologic units in the MHVC have been characterized by photogeologic and compositional analyses. The region has been studied using images from the LRO NAC [3, 4], 9-band spectral data from Clementine [3, 8], and compositional analyses using data from the Moon Mineralogy Mapper [M<sup>3</sup>; 8,9,10]. The results from Clementine revealed similarity

of composition between volcanic domes and the plateau, but differences in the spectral response of the cones [8]. M<sup>3</sup> analysis revealed an abundance of olivine in the MHVC. The identification of olivine, a primitive mineral that is thought to have originated at depth within the lunar crust, has been problematic on the lunar surface because it is difficult to distinguish from volcanic glass in planetary spectral analysis [6]. The combination of spectral indices used here [6] can distinguish olivine from volcanic glass in M<sup>3</sup> data.

**Methods:** M<sup>3</sup> was an imaging spectrometer on the Chandrayaan-1 lunar orbiter operating in the visible to near-infrared (0.42μm-3.0μm). M<sup>3</sup> in global mode has a resolution of 140 m/pixel in 86 spectral channels [11]. M<sup>3</sup> collected data during two operational periods distinguished by changes in instrument temperature and viewing orientation. Data in this project was collected from operational periods 1B, 2A, 2B, and 2C. A M<sup>3</sup> map of the region was constructed (Figure 2) with bounds 300-312°E and 9-17°N. The continuum of each spectrum was removed [6, 7] using a linear convex hull with two segments between 0.6-2.6 μm. Spectral noise was reduced using a median filter and a boxcar smoothing algorithm, both with widths of 5 channels.

**Figure 2:** Composite M<sup>3</sup> view (R=glass band depth, G=



1μm band center, B=2μm band center) of the MHVC superimposed on the LRO Wide Angle Camera (WAC) mosaic. Horizontal variability across M<sup>3</sup> frames is due to changes in resolution and sensitivity between observations. Boxes indicate locations of spectra in Figure 3.

Spectral parameters were applied to our M<sup>3</sup> map. Our glass spectral parameter detects the wings of the glass iron absorption band, which is centered at much longer wavelengths than other Fe-bearing minerals, based on the average band depth below the continuum at 1.15, 1.18, and 1.20 μm [14]. These maps are shown along with topography from LOLA Figure 1.

**Preliminary Results:** In the  $M^3$  color composite (Figure 2), red represents the glass band depth, green is the  $1\mu\text{m}$  band center, and blue is the  $2\mu\text{m}$  band center. Yellow/green colors mark the possible locations of glass-rich deposits associated with pyroclastic volcanism mixed with orthopyroxene (OPX). The widespread distribution suggests that volatile-rich eruptions may have played a prominent role in the emplacement of volcanic features of the MHVC. Figure 3 compares spectra collected from locations in Figures 1 and 2 to laboratory spectra of glass and orthopyroxene. Both glass and orthopyroxene display  $1\mu\text{m}$  and  $2\mu\text{m}$  bands with differing band centers. Movement in the  $2\mu\text{m}$  band shows the addition of another phase to the OPX, most likely glass.

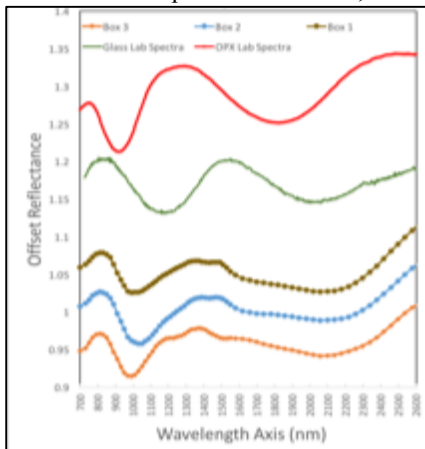


**Figure 3:** The bottom three spectra were collected from  $M^3$  data of the volcanic domes within the boxes in figures 1 and 2. The spectra can be compared to laboratory spectra of glass (green) and OPX (red). The similarities and differences between the spectra are evident in the  $1$  and  $2\mu\text{m}$  band centers and asymmetries.

More detailed examination of the color composite (Figure 2) shows an increased concentration of glass in the locations of several volcanic domes. These domes have been interpreted as volcanic shield volcanoes responsible for effusive eruptions in the region, and have been related to nearby volcanic cones [4]. Effusive eruptions cool slowly and are not usually glass rich. In the composite image (Figure 2), the raised domes appear to be comprised of mixtures of glass and orthopyroxene represented by the yellow and green combination which is differentiable from the areas between the raised domes. This mixture of phases is similar to that observed within the Aristarchus LPD located to the north of Marius Hills [12]. The similarity is intriguing because Aristarchus does not contain dome morphology and the source of the LPD is not known.

The cones at MHVC have been interpreted as volcanic cinder cones based on their morphologies [1,2,4]. Cinder cones would be expected to have associated glass deposits because they form via explosive eruptions

[13]. The  $M^3$  glass band depth map (Figure 4) shows three examples of cinder cones in the MHVC. These data clearly show that surface deposits associated with the cinder cones are more glass rich, with 3% to 7.5% glass band depths, than the surrounding area and their cone-shaped morphologies are distinguishable.

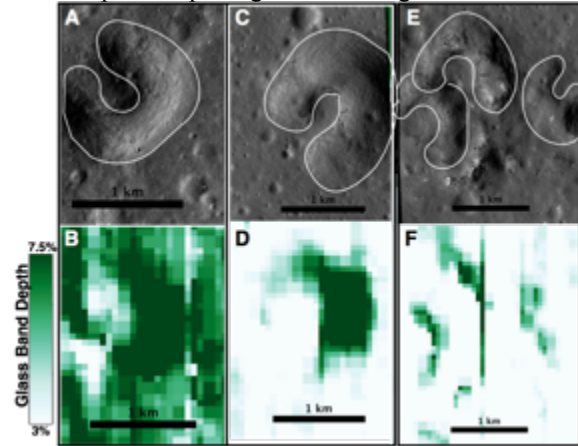


**Figure 4:** LRO Narrow Angle Camera (NAC) views and  $M^3$  derived glass band depth maps for several cinder cones at MHVC. The cinder cone morphologies can be seen in the associated glass maps as would be expected for cinder cones.

**Summary and Future Work:** Our results indicate that pyroclastic volcanism was common at MHVC, More detailed morphologic mapping of the plateau is needed to clarify the relationship of the glass presence to specific volcanic features. The MHVC bears numerous similarities to the Aristarchus region. Located south of Aristarchus, the volcanic features on the MHVC appear to be of similar composition with volcanic glass on the raised orthopyroxene rich plateau. The plateaus in these regions are hypothesized to be uplifted in association with the Imbrium impact or possibly large shield volcanoes [2,15], this suggests that they may be related as part of the same circum-Imbrium volcano-tectonic field.

**References:** [1] Whitford-Stark and Head (1977), LPSC, 8th, 2705–2724. [2] McCauley 1967, McCauley, J. F., U.S. Geol. Surv. Misc. Invest. [3] Gustafson et al., (2012), *J. Geophys. Res. Planets*, 116(E6), E00G13 [4] Lawrence et al., (2013), *J. Geophys. Res. Planets*, 118, 615–634. [5] Gaddis, L.R. et al. (2003) *Icarus*, 161:2, 262–280. [6] Horgan et al., 2014, *Icarus*, 234(C), 132–154. [7] Bennett et al. (2016) *Icarus*, 273, 296–314. [8] Weitz et al., (1999), *J. Geophys. Res. Planets*, 104(E8), 18933–18956. [9] Besse et al., (2011), *J. Geophys. Res. Planets*, 116, E00G13. [10] Heather et al., (2003), *J. Geophys. Res. Planets*, 108(E3), 5017 [11] Pieters, C. M. et al. (2009) *Curr. Sci*, 96:4, 500–505 [12] McBride et al (2016) LPSC, 47, 3052. [13] Wood (1979) LPSC, 10, 1370. [14] Gaddis et al. (2016), LPSC, 47, 2065. [15] Spudis et al., (2013), *J. Geophys. Res.*, 118, 1–19.